--15

SAND--91-1756C

DE91 018814

OVERLOOKED FUNDAMENTALS OF RESISTANCE WELDING

G.A. Knorovsky
Sandia National Laboratories
Albuquerque, NM 87185

Abstract

Resistance Welding (RW) has been known for about a century and in common use for much of that time. Much knowledge has been accumulated concerning many aspects of the process. However, upon examining contemporary RW handbooks, a few subjects that have been "overlooked" were found. Usually, this oversight will not be important; however, when the RW process is being applied at its limits, these factors may become critical. In this paper we will discuss such "overlooked" factors as the Peltier and Thomson effects, and the dynamics of welding head motions and how they are affected by the current pulse. Examples taken from sheet metal and microwelding applications will be given as examples.

Introduction

Resistance Welding (RW) has been practiced for over one hundred years since its invention by Elihu Thomson. In that period, RW has developed into a major industrial process, and a considerable body of knowledge about many aspects of the process has developed. However, despite RW's being one of the most commonplace welding processes, and in many ways one of the simplest, a number of aspects are neglected in standard references on the process, such as the AWS Welding Handbook(1) and the RWMA Resistance Welding Handbook(2).

In this work, two of these aspects will be discussed. The first relates to the fact that not all of the heating in resistance welding is generated by resistance heating. In at least one important class of welds, a significant portion of heat is controlled by thermoelectric effects, also known as the Peltier and Thomson effects, rather than the more familiar Joule (I^2R) effect.

The second neglected fundamental deals with the requirements for assuring good electrode "follow" behavior. Normally, the recommended design to achieve good follow behavior involves the

---

use of "low inertia" welding heads. In reality, because a resistance welding head acts like a sprung mass, much like an automobile suspension system, a more complicated specification involving damping is necessary. An appropriate analogy would be driving a high performance sportscar on a bumpy road with its shock absorbers (dampers) removed.

Relative Contributions of the Joule, Peltier, and Thomson Effects

Because of their common use in industry, thermocouples and the thermocouple (or Seebeck) effect are relatively well known. In this phenomenon, a difference in temperature between the ends of a bimetallic pair of conductors connected in an electric circuit causes an electric potential difference to occur. Less well known is the inverse effect, the Peltier effect, where a current flow through a bimetallic junction causes energy to be absorbed or released at that junction. The Thomson effect (named after William Thomson, Lord Kelvin, not Elihu Thomson) is similar, but instead acts in a single conductor, and refers to heat absorbed or released when electric current flows through a conductor which contains a temperature gradient. The explanation of these effects lies in the conservation of energy and how the energy levels of conduction electrons vary with location (when crossing a bimetallic interface) and temperature.

An easily understood analogy for the Peltier effect lies in the energy of a canoe going over a river rapids, or a salmon struggling upstream to spawn. Think of the river levels as corresponding to the differing conduction electron energy levels of the two materials joined at the "rapids". As the canoe or salmon (a conduction electron) changes levels, it also gains or loses potential energy. Since the kinetic energy of the electron is essentially constant, and governed by the (current) flow, the potential energy gained or lost is converted into a thermal effect. Mathematically(3), the Peltier effect heat is expressed by:

$$dQ_p/dt = -\Pi_{ab}J$$

where dQ_P/dt is the rate of heat released (i.e. the thermal power) per unit area due to current flow from material a to material b, Π_{ab} is the Peltier coefficient, and J is the current density. Note that unlike the Joule heating effect, given by:

$$dQ_j/dt = J^2\rho$$

where dQ_j/dt is the power produced per unit volume by current flowing through a conductor of resistivity ρ, in the Peltier effect the value of current density is not squared, and hence the heat effect can be either positive (release) or negative (absorption), and further, reverses sign as the current flow direction reverses. This is the explanation why direct current resistance welds are sometimes polarity sensitive(4). It also offers an explanation as to why one electrode usually wears faster than its nominally identical counterelectrode.

The Peltier coefficient is related to the Seebeck coefficient (the proportionality constant $S_{ab} = dV/dT$ which relates output voltage to hot vs cold junction temperature difference for a thermocouple of materials a & b) by:

$$\Pi_{ab} = TS_{ab}$$

Hence the Peltier effect tends to be more important at higher temperatures. Finally, while the Peltier coefficient for a bimetal pair is governed by both members of the junction, data is compiled for individual materials. The paired material coefficient is obtained by subtracting values of the individual material coefficients:

$$S_{ab} = S_b - S_a$$

Data is available(3) for pure materials, thermocouple materials, and other materials where the thermoelectric coefficients have been used to measure solid state phenomena (dilute magnetic alloys). Unfortunately, thermoelectric data is not available for many commonly resistance welded materials such as aluminum alloys and stainless steels.

The Thomson effect is governed by:

$$dQ_T/dt = -\mu\mathbf{J}\cdot\nabla\mathbf{T}$$

where dQ_T/dt is the rate of heat released per unit volume, μ is the Thomson coefficient, **J** is the current density (a vector) and $\nabla\mathbf{T}$ is the temperature gradient (also a vector). Absorption of heat (dQ_T/dt negative) occurs if the current flow and thermal gradient vectors are parallel and μ is positive. Of the three thermoelectric effect coefficients, the Thomson coefficient is the only one which can be measured directly for a single material. The three thermoelectric coefficients can be shown to be interrelated by:

$$\mu = TdS/dT \quad \text{and} \quad \Pi = TS$$

where T is the absolute temperature. Note that these relationships of the Thomson coefficient to the other thermoelectric coefficients, (which really are only measureable in pairs), allow values of S and Π for single materials to be tabulated without arbitrarily defining one material to be of zero potential.

Given these three effects, what are their relative contributions for typical resistance welding scenarios? Because the Peltier effect is two dimensional and the Joule and Thomson effects are three dimensional, it is difficult to compare all three directly. It is possible to compare the Joule and Thomson effects, as they can be combined into a single equation relating rate of heat production per unit volume to current:

$$dQ/dt = \rho J^2 - \mu J \nabla T$$

or alternatively:

$$dQ/dt = J(\rho J - \mu \nabla T)$$

Typical values of ρ range from ~1 to ~100 $\mu\Omega$cm for metals(5), with Cu at room temperature having a value of 1.6 and Fe at 1000°C a value of 110 (data beyond 1000°C is hard to obtain). With typical welding currents, J has values in the range of 10-100 kAmps/cm^2(6), and the product ρJ would then tend to range between 0.01-10 V/cm. Likewise, the absolute value of μ typically ranges from about 1.5 to 35 μV/°K, while ∇T ranges from 0 to about 50,000 °K/cm, and the product can vary from zero to ~1.5 V/cm. Comparing the relative sizes of these two products, it is seen that under certain circumstances the Joule heating can overwhelm the Thomson heating (or cooling), while in others the two can be comparable in magnitude. Since μ and ρ are both of approximately the same magnitude for common metals, whether the current density or the thermal gradient is larger will determine which effect predominates (at least when using V-A-Ω-cm-K units). Another important consideration is that both effects cause voltage drops, which need to be isolated when trying to measure apparent resistance across a weld. In symmetrical geometries with differential measurements the Thomson effect voltage should cancel; however, the Peltier effect may cause assymetrical thermal gradients in apparently symmetrical geometries.

To compare the Joule and Peltier effects, it is necessary to realize that the Peltier heat is not a function of the volume of the material that the current is flowing through. That is, if a given current density flows through two sheets of steel, one of which is 10 cm thick, and the other 1 cm, the Joule heat released will be 10 times as great in the former. On the other hand, if the two sheets are different materials, and a Peltier effect occurs, it will be the same no matter how thick the materials are. Thus a good comparison between Joule and Peltier heating is to find the thickness of materials needed to release the same amount of energy via either mechanism. This is expressed by the equality:

$$| dQ_p/dt \text{ (in J/cm}^2\text{-sec) } | = dQ_j/dt \text{ (in J/cm}^3\text{-sec) } \Delta z$$

where Δz is the overall couple thickness in cm, or alternatively:

$$| -\Pi_{ab} J | = J^2(\rho_a \Delta z_a + \rho_b \Delta z_b) = J^2(\rho_a + \rho_b)\Delta z/2$$

where the subscripts refer to the two materials in the couple (each of equal thickness), and thus:

$$\Pi_{ab} = J(\rho_a + \rho_b)\Delta z/2$$

and finally:

$$\Delta z = 2\Pi_{ab} / [J(\rho_a + \rho_b)]$$

Picking an Fe/Cu couple at 0 and 1000°C, the appropriate constants and calculated Δz values are compiled in Table I.

Table I Resistivities, Peltier Coefficients and Calculated Equivalent Joule Heat Thickness for Fe/Cu Couple.

Temperature	0°C			1000°		
Coefficient / Metal	ρ ($\mu\Omega$cm)	Π (μV)	Δz (cm)	ρ	Π	Δz
Fe	8.59	3,986		112	-8,020	
Cu	1.56	467		9.3	8,990	
J (A/cm^2) 10,000			0.070			0.028
100,000			0.007			0.0028

Table II Resistivities, Peltier Coefficients and Calculated Equivalent Joule Heat Thickness for Ni/Mo Couple.

Temperature	0°C			1000°		
Coefficient / Metal	ρ ($\mu\Omega$cm)	Π (μV)	Δz (cm)	ρ	Π	Δz

Ni	6.4	-4,870		48.1	-48,100	
Mo	4.6	1,256		16.1	20,500	
J (A/cm^2) 10,000			0.112			0.214
100,000			0.011			0.021

It is seen that while the thicknesses calculated are small, they are non-negligible. Also, the thickness is inversely proportional to current density. For the example chosen, it appears that the effect decreases at elevated temperatures; this is not necessarily always the case. For example, if a Ni/Mo couple is chosen, both of which have relatively large (and opposite sign) Peltier coefficients, the appropriate constants and calculated Δz values are compiled in Table II. At 1000°C the Peltier heat for this couple is about twice as important as at 0°C. Again, note that the Peltier effect coefficient has units of a voltage, and it too can lead to measurement errors in non-symmetrical situations.

To combine all three effects, two different situations will be examined, one typical of an industrial sheet metal type weld (though we'll assume a DC power supply, rather than the more typical AC) and one typical of an electrical interconnection. For the sheet metal application we'll assume that two sheets of 1mm thick low carbon steel are being joined, and for the electrical application we'll assume that a 0.1mm Ni ribbon is being joined to a 3mm diameter by 4mm high Mo terminal pin (typical of long life Li-containing D-size battery).

Case I (automotive)

The RWMA recommended practice(2) suggests an electrode contact spot of 0.25 inch (0.635 cm) diameter, 10 cycles of weld current of 9,500 Amps, using RWMA Class 2 electrodes and 500 lbs (2,200 N) electrode force. This corresponds to a current density of 30,000 $Amps/cm^2$. There is no data for the thermoelectric coefficients of Class 2 electrode material, so we will use data for pure Cu. Similarly, we shall use data for pure Fe instead of low carbon steel. In the table below, values of heat generation are calculated for volumes of 1 cm^2 cross-section of the appropriate length. Only the left half of the weld geometry is shown. The right half should be symmetric for the Joule effect, and anti-symmetric for the Peltier and Thomson effects. We will assume temperature distributions and make calculations of heat effects at three points in time during the weld. At the beginning of the weld the initial temperature is uniform at 0°C. At the start of melting, a linear temperature distribution exists between the central temperature at 1500 °C and the electrode/material interface at 200°C. This then reduces linearly to

0°C in the electrode material over a distance of 6.35 mm. At the end of current flow, the melting isotherm is located 3/4 of the part thickness from the centerline (the fusion zone is considered to be isothermal at 1500°C), the electrode/material interface is at 400°C, and a linear temperature gradient exists between these points. The electrode material is again assumed to cool linearly with distance to 0°C over 6.35 mm. These scenarios are illustrated in Figure 1; the temperatures chosen at the electrode/part interface correspond to available data(7). Positive current is assumed to flow from left to right. A negative sign implies heat is absorbed; positive that heat is generated. The actual values used for the Thomson and Joule coefficients are averages over the temperature ranges applicable. If the coefficient was not well-behaved (i.e. not continuous), an interval over which an average value was computed is noted. Wherever a calculation temperature exceeds 1000°C it has been extrapolated by curve fitting (except for the resistivity of Fe).

Note that the signs of all Peltier and Thomson terms are reversed on the other side of the center line (C_L) and that there is no Peltier effect at the Fe/Fe interface. Also note that because of the non-monotonic temperature dependence of the Peltier and Thomson coefficients of Fe, the Peltier and Thomson heat effects behave in a complex manner with temperature. Observing the results in Table III, it is clear that the Joule effect is quite dominant under all conditions, with the thermoelectric effects never consituting more than a relatively small fraction of the overall heat production. From the viewpoint of efficiency, it is interesting to note that at the beginning of the weld more heat is generated in the electrodes than in the weldment!

Case II (battery terminal)

Experiments in our laboratory designed to develop a weld schedule for this connection suggest that a current of 1800 Amps through an electrode contact spot 2 mm in diameter (~60,000 Amp/cm^2) for a time period of 20 ms will yield successful welds. A Mo electrode (negative polarity) contacts the Ni ribbon, and a Cu alloy electrode contacts the Mo pin. 50 N of electrode force are used. Because the weld geometry is not symmetrical, we show the entire geometrical sequence in Table IV. Again, the values of power are calculated per cm^2 cross-section of appropriate length with temperatures assumed as follows. Initially a uniform temperature of 0°C exists; at the start of melting the Ni/Mo weld interface is at 1450°C, while the Mo/Ni electrode interface is at 1000°C and the Mo/Cu weld interface is at

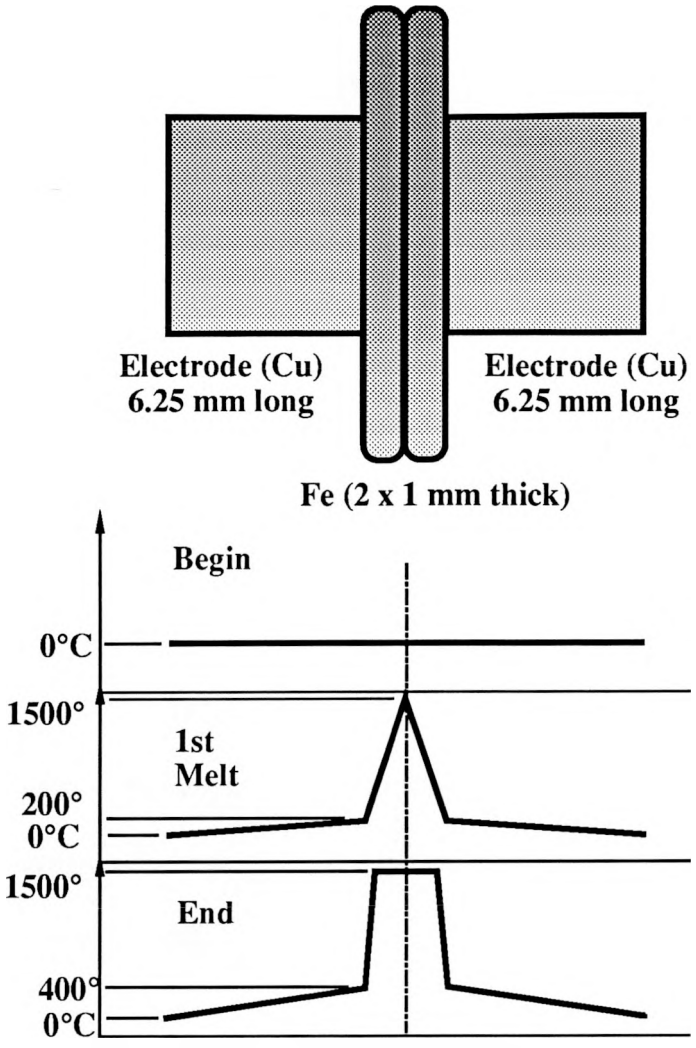

Figure 1: Case I geometry and thermal profiles.

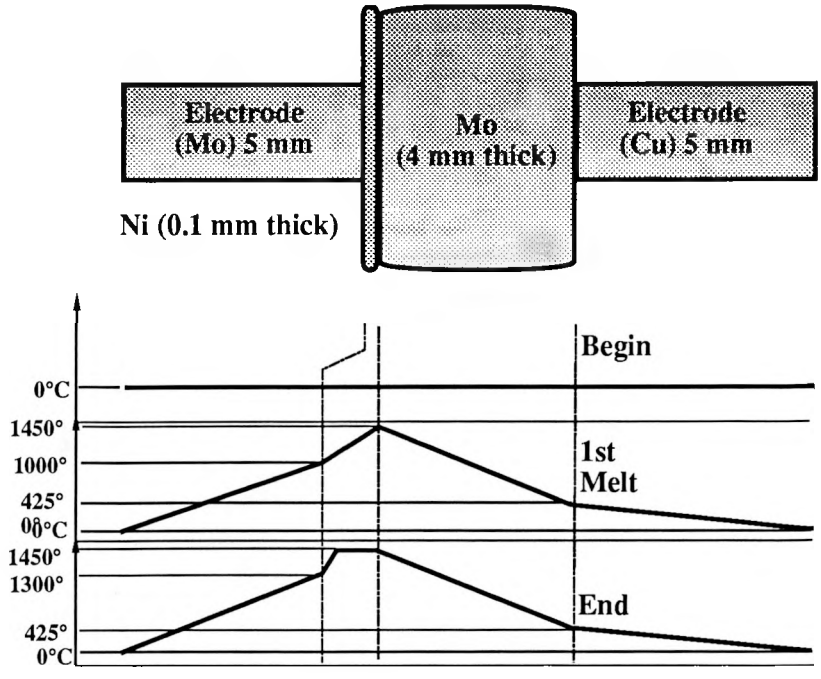

Figure 2: Case II geometry and thermal profiles.

425°C (the electrodes linearly cool to 0°C over a distance of 5 mm). At the end of current flow melting has propagated from the Ni/Mo interface into the Ni ribbon to a distance of 0.075 mm, the Mo/Ni electrode interface is at 1300°C, and the Mo/Cu electrode remains at 425°C. Interpolations between the points given are linear (see Figure 2), and the values calculated refer to averaged coefficients over the temperature ranges where gradients exist. Wherever a calculation temperature exceeds 1000°C it has been extrapolated by curve fitting (except for the resistivity of Mo). These simplified assumptions are based upon some finite difference calculations(8), which were qualitatively verified by metallography. In comparison with Case 1, these results are quite different. First, in contrast to the

Table III Calculated Relative Powers of Thermoelectric and Joule Effects for Case I.

Effect:	Time:	Location:			C_L
		Cu Electrode	Interface	Fe solid	Fe liquid
Joule	begin	890 J/s		770	-
	1st melt	960		3800	0
	end	1670		1710	7500
Peltier	begin		-105		
	1st melt		-34		
	end		157		
Thomson	begin	0		0	-

	1st melt	-12		176 (200-577°C) -195 (577-910) -157 (910-1500)	0
	end	-30		31 (400-577°C) -195 (577-910) -157 (910-1500)	0

automotive case, where the electrodes were generally much better conductors than the weldment, here one of the electrodes dissipates nearly as much heat as the Mo terminal. This isn't surprising, as it is the same material, sees about the same temperature range, and is about the same length. The data in Table IV are not normalized for length (only cross section) so the large thickness disparity between the electrodes and terminal pin versus the Ni ribbon (5 mm, 4 mm, and 0.1mm, respectively) makes it hard to see that the Peltier and Thomson effects are really quite significant in this case. Dividing the electrode entries by 50, and the terminal pin entries by 40 does this, allowing the heating contributions to be compared on an equivolume basis. Such a comparison is fair only at the beginning, because otherwise the resistivity change with temperature is not correctly factored in. The resistivity values used to calculate the electrode and terminal entries in Table IV were averaged over the temperature intervals shown in Figure 2, while the temperatures at the Ni/Mo and Mo/Ni interfaces are much higher, and hence the resistivity used to calculate the Joule effect heating should be higher. For the case of Mo, the resistivity changes by about an order of magnitude between 0 and 1450°C. A reasonable comparison for the 1st melt and end values can then be made by multiplying the "begin" value by the resistivity change with temperature divided by the thickness disparity, 10x/50x (or 10x/40x for the terminal) to see the Mo Joule heating effect at temperatures near the melting point of Ni. For example, at the end of the weld, it is calculated that about 1850 J/sec of heat are being supplied by Joule heating in a 0.1mm thickness of the Mo electrode and terminal on either side of the Ni ribbon. The Ni ribbon itself is providing about 2180 J/sec. The Peltier effect is providing 6400 J/sec of heat at the ribbon/terminal interface, and 5600 J/sec of cooling at the electrode/ribbon interface. It is clear that this will have a substantial effect on the thermal balance. The Thomson effect is also significant compared to Joule heating before the thermal gradients in the Ni ribbon begin to diminish.

Effect of the Interfacial Resistance

The interfacial resistance must also be considered to complete the analysis. Data from (6) suggests that the surface contact resistivity

for Cu alloy vs mild steel at room temperature is on the order of 1.25×10^{-4} ohm/in^2. (or 7.7×10^{-4} ohm/cm^2). This suggests that the initial heating rate at the surface (per cm^2) for Case I is of the order of 700,000 J/sec! This resistance would correspond to that of an Fe bar of 1 cm^2 area nearly 90 cm long. Clearly, this rate cannot be sustained for long, as the surface asperities which constrict the current and are the main cause of surface resistivity will rapidly heat and collapse, causing the surface resistivity to drop to a small value. Nevertheless, it is clear that the early stages of heating are overwhelmingly controlled by surface resistance. The Ni-to-Mo weld finite difference calculations mentioned earlier which incorporated the Joule and Peltier effects also incorporated a surface resistivity term. These results, plotted in Figure 3, clearly demonstrate the importance of both the surface resistance and the Peltier effect. Temperature dependent physical properties were used, except the Seebeck coeffient (which controls the Peltier coefficient) was held constant at an average value. Additionally, the surface resistivity (chosen as 100 $\mu\Omega$/cm^2) was set to zero when the interface warmed to half the homologous melting point. The calculated interfacial temperatures (both weld and electrode) show clearly that the initial temperature rise is independent of the polarity chosen, but that subsequent to reaching the melting temperature, the

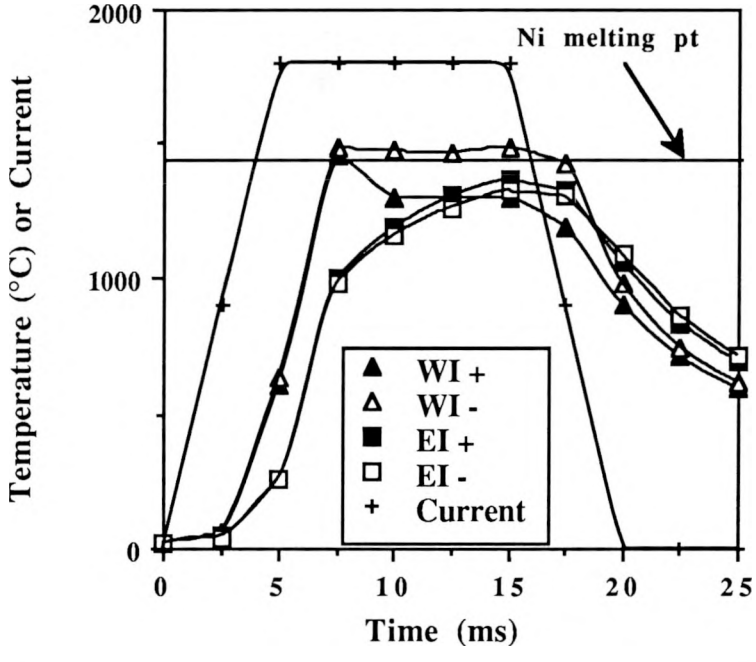

Figure 3: Calculated temperatures at weld interface (WI) and electrode interfaces (EI) for geometry shown in Figure 2 as a function of Mo electrode polarity.

Peltier effect becomes evident. We found that after the initial transient, the weld interface temperture for the wrong choice of polarity was less than the electrode interface temperature!

Dynamics of Resistance Weld Heads

In the introduction, we asserted via an automotive analogy that low inertia is an insufficient design requirement for acceptable follow in

resistance weld head design. Figure 4 is a simplified schematic of an hypothetical resistance welding head, showing the various masses, springs and bearings. For complex real systems analytical calculation of the motion of a given point or points is a complex and time consuming procedure, even using available powerful finite element analysis programs. Indeed, sometimes the best procedure is to perform an experimental modal analysis, and use the results to understand the various motions possible, their resonant frequencies, and their relative importance. This procedure, while involved, is greatly facilitated by the computerized analysis and modelling procedures now available to vibration specialists. Certainly, when the resistance welders commonly used in industry were developed, these procedures were far less common, and it is possible that modal analyses made on small welding heads in our laboratory are some of the first performed. However, by examining the dynamic behavior of a simple linear single degree of freedom spring-mass-damper system, we can gain considerable insight into the behavior of more complex

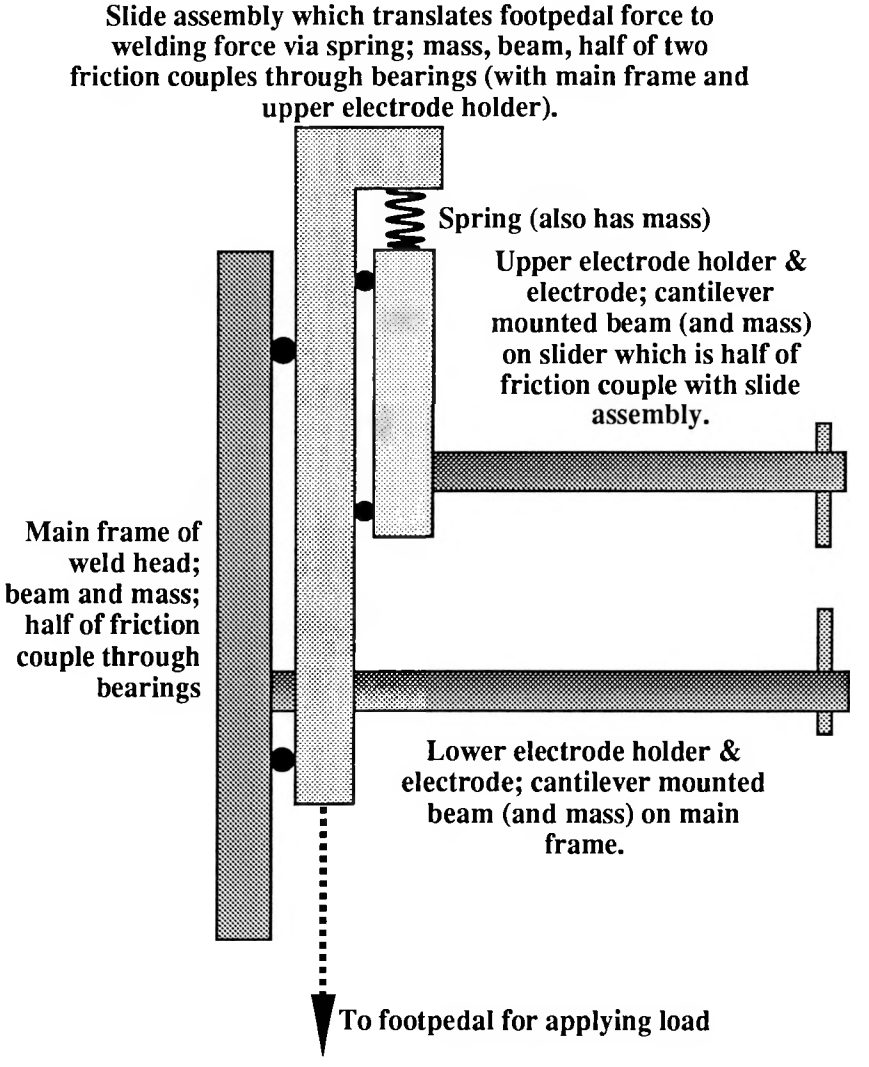

Figure 4: Schematic of typical small resistance weld head

systems. The mathematical analysis of such a system is well-developed and tractable, yet exhibits much of the character of the behavior of more complex systems. It is often observed that in multiple degree of freedom systems, the lowest order modes are dominant.

There are two important regimes in vibration analysis: forced and free. Forced vibration refers to a regime where the system is driven by a periodic external force. If the periodic force is sinusoidal this is referred to as harmonic motion. An AC type welder, where current pulses occur at periodic intervals, would exemplify this regime. Free vibration refers to a situation where the system is given some initial stimulus to which it responds. A capacitive discharge or DC welder is more characteristic of this type. Referring to the simple single degree of freedom system, the simplest type of free vibration to analyze is one where the system is removed from equilibrium (by stretching or compressing the spring) and then released. The solution of Newton's second law of motion in the form:

$$m \cdot (d^2x / dt^2) + b \cdot (dx/dt) + k \cdot x = 0$$

where m = mass, b = damping coefficient, k = spring constant, and subject to the appropriate boundary conditions, will decribe how the system evolves with time. Many elementary texts on differential equations, for example (9), use this as an introductory example of Laplace transformation solution methods. The behavior of the system under conditions of no damping, critical damping, and overdamping are shown in Figure 5. While the rate of return to the equilibrium condition is fastest for the no damping case, it is clearly unacceptable because of oscillation. This oscillation takes place at the so-called natural frequency of the system, which is given by:

$$f_n = (1/2\pi) \cdot (k / m)^{0.5}$$

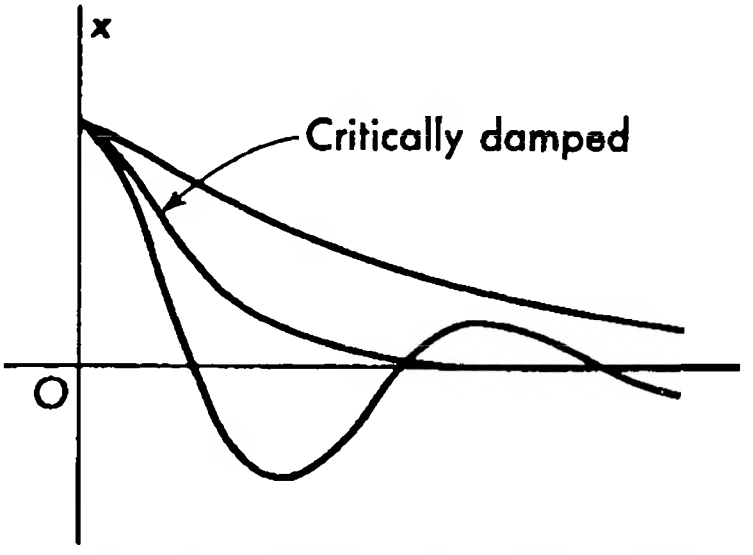

Figure 5: Free response of system with variable damping. Upper curve is over damped, oscillatory curve is underdamped.

For cases where less than a critical amount of damping takes place, oscillatory behavior still takes place, but the system eventually returns to equilibrium, and the damped natural frequency is slightly modified by the damping term:

$$f_d = f_n (1-\zeta^2)^{0.5}$$

where $\zeta = b /(2[km]^{0.5})$. It can be shown that the logarithm of the ratio of sucessive amplitudes (the so-called logarithmic decrement ; $\delta = \log_{10} (\Delta x_1/\Delta x_2)$, where Δx_i is the peak displacement from equilibrium for swing "i" in a given direction) can be used to conveniently measure the damping in a system via the equation:

$$\delta = \log_{10} (\Delta x_i/\Delta x_{i+1}) = 2\pi\zeta / [(1-\zeta^2)^{0.5}]$$

which simplifies to $\delta = 2\pi\zeta$ for $\zeta \sim 0.3$ or less.

When the critical amount of damping is present ($\zeta = 1$), oscillatory motion ceases, the system returns to equilibrium in the shortest period of time, and the natural frequency concept becomes useless. Higher values of damping merely slow the return to equilibrium down. Measurement of a typical small resistance welding head in our laboratory gave a value of $\zeta \sim 0.05$.

The next most complex step involves shocking a system initially at equilibrium. If the shock involves applying a step function force (F_o) it may be shown (10) that the system responds as shown in

Figure 6. This situation is very close to what happens in a resistance welder, except that the force applied by the thermal expansion of the sample is not a square wave, and it decays to zero after some period of time. The ordinate of Figure 5 is expressed in multiples of the equilibrium static displacement that the step force would produce. For insufficient damping, the dynamic response is nearly twice the static displacement which should result. Another important method of displaying the resulting displacement of a system which has been shocked is the response spectrum curve. This shows the maximum displacement which will occur sometime during the response of an undamped single degree of freedom system (though it does not show actual displacement versus time) as

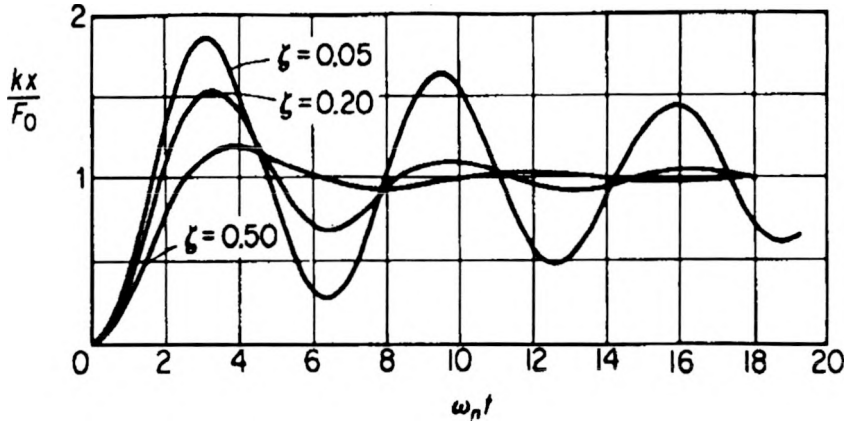

Figure 6: Time response of system to step function load F_o applied at time zero. ω_n is $2\pi f_n$.

the time of application of the shock varies with respect to the natural period (inverse of the natural frequency) of the system. The response spectrum diagram of a half cycle sinusoid is shown in Figure 7. It is clear that in order to respond in an accurate manner (i.e. near the static response value or ordinate = 1) one must choose a value of $t/\tau_n > 2.3$. The value where $t/\tau_n = 1/3$ apparently gives the correct response magnitude, but it is delayed in time, with the response being achieved long after the shock is over. The implication of these diagrams (an excellent compilation is given in (11) along with actual time response curves) is that the time of application of the shock must be long with comparison to the natural period of response of the system. Furthermore, gentler shocks are more accurately followed, and the effect of damping is generally positive in controlling the overshoot of the system (as long as it is not excessive).

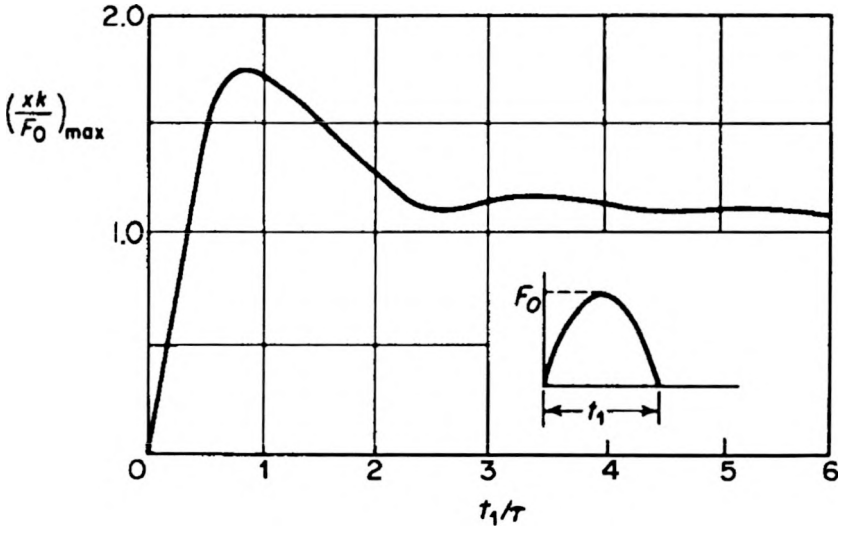

Figure 7: Response spectrum diagram to haversine force input (shown inset). τ is the natural period of the system.

It has been known for many years in the field of camshaft design that the third derivative of displacement (sometimes called the "jerk") must be controlled(12) in order to have a positionally accurate

motion control not prone to excessive vibration. (By making the assumptions of uniform I^2R heating and R linearly increasing with temperature it is possible to relate expansion vs time to current vs time; from which it can be shown that the initial third derivative of the displacement is proportional to the square of the slope of current vs time). Also important is a cam ramp time which is long in comparison to the natural period of the cam follower mechanism, and a cam that is stiff enough to resist the force applied to it by the follower. Poor dynamic design of a cam and follower can lead to follower "jumping" or loss of control, even when the spring loaded follower should be able to accelerate fast enough to follow the nominal acceleration profile of the cam. One other desirable feature is that enough damping must be present to damp out any vibrations generated before the system has to actuate again (i.e. during the "dwell" time when the cam is not actively controlling the motion of the follower). Returning to resistance welding, capacitive discharge type power supplies provide a very difficult shock load for a mechanical system to follow. From measurements made on our typical small welding head, the compliance and mass of the upper arm and its mounting slide result in a calculated natural frequency of only 25 Hz. However, this assumes that the slide carrying the upper electrode can actually move during the period of the weld. If one assumes a cantilever mount (i.e. the slide mount essentially remains motionless during the force application period), and relies on the elastic deflection of the electrode arm to follow the part expansion, then the natural frequency calculated from beam theory(10) is about 2.5 kHz. For a load application period of a few (1 to 5) milliseconds, this gives a ratio of t/τ_n of (0.001to 0.005) / (1/ 2,500) = 2.5 to 12.5 which is excellent. Excellent, that is, for a gentle half sinusoid load profile (or the even gentler classical cycloidal motion typical of camshafts). However, the deflection which must be accomodated by elastic bending of the electrode holder will cause the opposed electrodes to lose parallelism (like a rocker type head, which the slide type head was supposed to improve upon), and hence promote spatter because of non-uniform loading of the pressurized molten zone.

Even though forced vibrations have not been discussed, it is clear that for AC type power supplies, the natural mechanical response frequency of the system must not be too near twice the power frequency or any of its harmonics if a resonance situation is to be avoided. It is unfortunate that SCR's do not chop the tails off of sinsoidal current pulses rather than the beginnings, as chopped AC current pulses are clearly not a gentle load to follow. Fortunately each one is a relatively small contribution to the overall heat input.

To summarize, it is recommended that Resistance welder power supply and head designers should take a page from the book of camshaft designers. They should attempt to better tailor the electrical pulse (and the expansion resulting) to the capabilities of the mechanical system which must control it. Additionally, the effect of

damping on the mechanical response of a resistance weld head needs to be further investigated if our initial measurements of it are indicative of general practice.

Summary

In this work certain important but often overlooked aspects of resistance welding have been discussed. Joule heating due to both both surface and volume resistivities has been compared to Peltier and Thomson heat effects for two different situations. In one case the Joule effect is predominant, and in the other the Peltier effect has an important effect on heat generation. This has served to illustrate under what conditions the thermoelectric effects need to be considered. Concepts of dynamic response of mechanical systems to shocks and mechanical design procedures more commonly applied to camshafts have been applied to resistance welding heads. These illustrate that low inertia design by itself is not enough to provide good follow behavior. Additional requirements for damping and tailoring the impulse by controlling the current vs time behavior have been highlighted.

Acknowledgments

I would like to acknowledge in particular the assistance of A.J. Russo for performing finite difference calculations incorporating the Peltier and Thomson effects, and Arlo R. Nord for conducting experimental modal vibration testing and analysis of resistance weld heads. This work performed at Sandia National Laboratories supported by the U.S. Department of Energy under contract number DE-AC04-76DP00789.

References

1. L.P. Connor, ed., Welding Handbook, Vol.2, 8th Edition, (Miami, FL: American Welding Society, 1991).
2. D. Giroux, et.al., eds., Resistance Welding Manual, 4th Ed, Philadelphia, PA: Resistance Welder Manufacturers' Association, 1989).
3. F.J.Blatt, P.A. Schroeder, C.L. Foiles, D. Greig, Thermoelectric Power of Metals, (New York, NY: Plenum Press, 1976).
4. S. Scholz, "An Investigation of the Influence of the Peltier Effect on Resistance Welds," Zeitschrift fuer Angewandte Physick, 12(3)(1960), 111-117
5. K.-H. Hellwege, O. Madelung, eds., Landolt-Bornstein, Numerical Data and Functional Relationships in Science and Technology, New Series, Group III: Crystal and Solid State Physics, Vol. 15, Metals: Electronic Transport Phenomena, (Berlin:Springer-Verlag, 1982).
6. H. Udin, E.R. Funk, J. Wulff, Welding for Engineers, (New York, NY, John Wiley and Sons, Inc., 1954).
7. E.W. Kim, T.J. Eager, "Measurement of Transient Temperature Response during Resistance Spot Welding," Welding Journal Res. Suppl., 68(8)(1989), 303-s-312-s.

8. A.J. Russo, private communications with author, Sandia National Laboratories, Albuquerque, NM, July-Dec. 1988.
9. E.D. Rainville, Elementary Differential Equations, 3rd Ed., (New York, NY: The Macmillan Co., 1964), 212-224.
10. William T. Thomson, Theory of Vibration with Applications, 3rd Ed., (Englewood Cliffs, NJ: Prentice Hall, 1988), 92.
11. C.M Harris, C.E. Crede, Shock and Vibration Handbook, 2nd Ed., (New York, NY: McGraw-Hill Book Co., 1976), Chapter 8.
12. M.P. Koster, Vibrations of Cam Mechanisms, (London, The Macmillan Press, Ltd., 1974).

Table IV Calculated Relative Powers of Thermoelectric and Joule Effects for Case II

Phenonemon	Time	Location						
		Mo Electrode	Interface	Ni solid	Ni liquid	Weld Interface	Mo	Interface	Cu Electrode
Joule Effect:	begin	9,300 J/s		230	-		7,400		2,800
	1st melt	33,000		2,000	-		43,000		5,600
	end	41,000		530	1,650		43,000		5,600
Peltier Effect:	begin		-370			370		-47	
	1st melt		-4,100			6,400		-450	
	end		-5,600			6,400		-450	
Thomson Effect:	begin	0		0	-		0		0
	1st melt	400 (0<T<760) -90 (760<T<1000)		-780	-		-370 (425<T<760) 1360 (760<T<1450)		-70

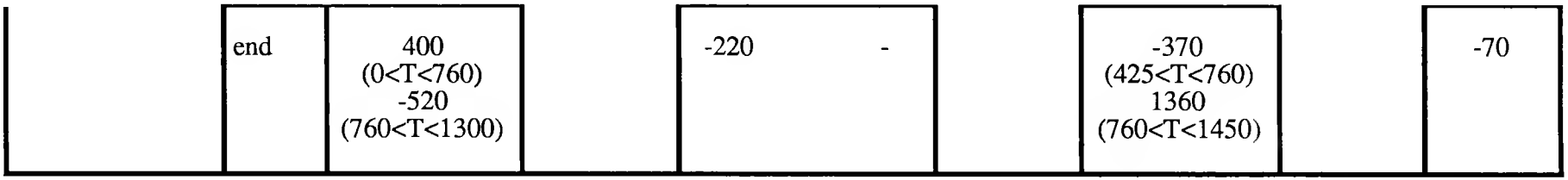
end
400
(0<T<760)
-520
(760<T<1300)
-220
-
-370
(425<T<760)
1360
(760<T<1450)
-70